

Spray evaporation study in high pressure combustion chamber using RANS computations

M. Chrigui, A. Sadiki, and J. Janicka

Institute of Energy and Power Plant Technology, Dept. of Mechanical Engineering
Technical University of Darmstadt, Petersenstr. 30, D-64287 Darmstadt, Germany
Fax: +496151166555 E-mail: mchrigui@ekt.tu-darmstadt.de

R. Eggels, T. Schilling, L. Rackwitz

Rolls-Royce Deutschland Ltd & Co KG
Eschenweg 11, D-15827 Dahlewitz, Germany

Introduction

Droplet evaporation in a high pressure and temperature environment is of great relevance for combustion devices such as gas turbines and diesel engines. The fuel is mostly injected into the combustion chamber in form of droplets, which undergo a sequence of phase transition (heating, evaporation), ignition and combustion processes at high pressure level. Droplet evaporation is therefore an essential process for fuel-oxidizer mixing and the subsequent mixture preparation.

Numerous theoretical studies have been carried out describing droplet evaporation. Faeth [1] considered in his work a simple approach to compute the evaporation and combustion of sprays. He applied the D2 model which has been widely used to describe the evaporation of fuel droplets. Droplets are heated till boiling temperature without any mass transfer, then an evaporation period at an almost constant temperature takes place. This model is suitable in case of small heating period time compared to the droplet life time. The Uniform Temperature model (UT model) [2] neglects the mass transport inside the droplet. Here the temperature variation in the interior of the droplet is assumed to be homogeneous. It has an unsteady behavior and it is accompanied with mass transition. Oefelein et al. [3] pointed out the behaviour of classical low-pressure and high-pressure evaporation models. They found out that the subsequent (high pressure) drop regression process is different from that in the subcritical (low-pressure) state. Prommersberger et al. [4] built an experimental setup where evaporation of free falling monodisperse droplets was investigated at high pressure; they then compared the experimental results with numerical calculations based on some equilibrium based droplet evaporation models. The convective transport of heat and mass at the droplet surface was calculated according to the film theory of Abramson and Sirignano [5] accounting for the molar mass fraction through the Clausius-Clapeyron equation. They achieved a best agreement with experimental data with the conduction limit model of Law and Sirignano (see in [2]), which assumes a diffusive heat and mass transport within the droplet.

The main focus of the present contribution is rather to investigate the droplet evaporation rate prior to combustion using an advanced RANS based spray module applied to a more complex configuration.

Theoretical-numerical framework

Droplet Tracking and Gas phase description

The spray module used in this work is based on an Eulerian-Lagrangian approach. For the Eulerian description of the turbulent gas phase, the simulation is performed using the three dimensional CFD-code FASTEST in which the equations are solved by finite volume method. The time integration is achieved implicitly with the Crank-Nicholson method while the diffusion terms are discretized with central schemes on a non orthogonal block structured grid. The velocity-pressure coupling is accomplished by a SIMPLE algorithm. The whole system is solved by the SIP-solver. For the Lagrangian phase, the code LAG3D-code is employed.

The droplet parcels are tracked in a time-accurate manner in a Lagrangian reference frame by solving their evolution equations, i.e., equations for the droplet position, velocity components, diameter (vaporization) and temperature (heating). A large number of parcels, representing in the polydispersed spray a number of real droplets with the same properties, are used in order to allow the consideration of droplet size distribution and to simulate the appropriate liquid mass flow rate at the injection locations. We do not consider the primary atomization and the spray formation. The motion equations include terms for the drag and the gravitational force. In order to simulate the dispersion of droplets and the interaction with the turbulent flow, the Markov-sequence model based on the calculation of Lagrangian and Eulerian correlations factors[6] is applied. The Lagrangian equations are discretized using first order scheme and solved explicitly.

The turbulent fluid phase is described in the frame of an Eulerian description. The standard k - ε turbulence model as well as Reynolds Stress Model have been chosen. To achieve the coupling between both phases a fully two-way coupling that additionally takes into account the effect of the presence of particles/droplets on the carrier phase is considered. This involves interaction terms in momentum, turbulence quantities, energy and mass conservation equations. The source terms for the gas phase are computed in each cell with the contributions of all the relevant droplets. Numerically, the interaction between the continuous and the dispersed phases consists in a coupling between the two codes involved. Following a steady method, after several iterations in time of the gas phase solver alone, the gas variables are kept frozen and all the droplets representing the entire spray are injected in the computational domain.

Droplet Evaporation Model

Even though the conduction limit model has provided good agreement in [4], this model is not considered here due to its high computational time consumption. The Uniform Temperature model [2] is rather used. As this model does not account for the gradient at the interior of the droplet, droplets are not discretized. Therefore this model does not require high computing time. A detailed description of the model can be found elsewhere [5, 8].

Configuration and flow conditions

The simulated configuration stems from the company Rolls Royce (RR) Deutschland. The combustion chamber BR710 consists of an annular combustor which is fired by 20 burners having a central fuel nozzle and two axial swirlers. For the numerical simulation only one sector of 18 degrees has been modeled. The single dome sector of 18° span includes swirler, which was accounted for by inlet boundary conditions, fuel nozzle on the inlet and a set of primary and secondary openings on the outer and inner walls (Figure 1).

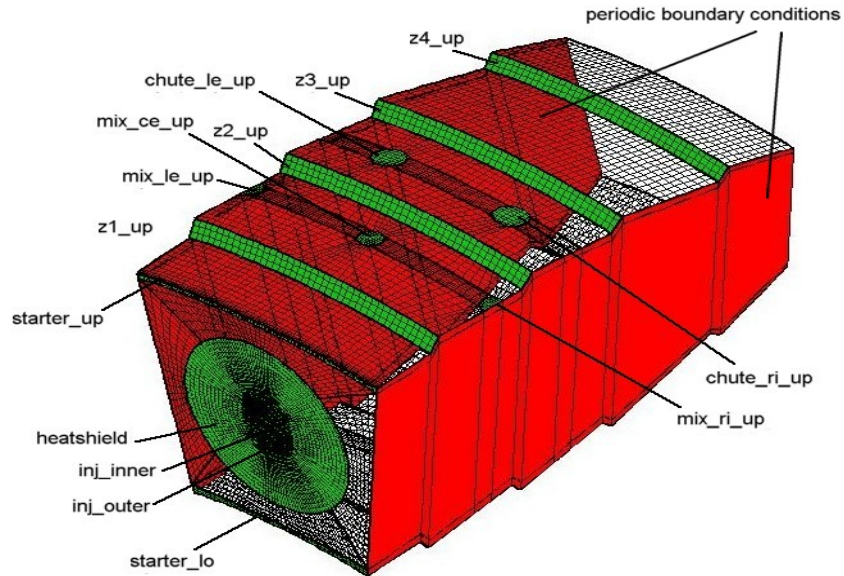


Figure 1: Single annular combustor geometry and inlets

The overall mesh for the single annular combustor without fuel injector is about 350 000 control volumes. The grid of the gas-turbine combustor sector has 99 multiply-connected domains, i.e., they consist of several separate flow-paths that interact with each other. Cartesian coordinates and hexahedral cells were used to generate the mesh. The boundaries specified at inlets include heatshields, starter and Z-ring cooling air, as well as primary and secondary air mixing ports.

The inlet boundary conditions for the combustion chamber corresponded to scaled take off conditions. The pressure was scaled to $P_{inl}=1241$ kPa according to experimental data carried out in a full annular combustor rig. The corresponding temperature $T_{inl}=842$ K. The mass flow boundary conditions for the gas phase were provided by measurements and estimated by a RR in house code.

The fuel injector exists of three different air swirlers, inner, outer and dome air swirler [7]. Each one is defined primarily by its effective area and its swirl angle. Additional swirling air is introduced by the heatshield inlets. The circumferential velocities are simply determined using the swirler vanes turning angels and the constant axial velocities, which are calculated from cold flow rig test measurements. Swirlers were not included in the computational domain, since no geometrical data was available. However, boundary conditions at the inlets were imposed by velocities profiles provided by RR.

Inlet conditions for the turbulent kinetic energy were calculated using a turbulence intensity of 10% of the resultant velocity through an inlet. For the Reynolds Stress Model, only main diagonal components were considered along with a turbulence intensity of 10%. Tangential components of the Reynolds stress tensor were set to zero.

The combustion chamber is operated with liquid kerosene at a pressure of 12.0 bars. However, kerosene is a multi-component fuel which typically consists of a mixture of about 10 hydrocarbons such as n-dodecane, alkyl derivatives of benzene, naphthalene and derivatives of naphthalene. As the model available is suitable for pure component droplets, we therefore substitute for the simulation kerosene fuel by dodecane $C_{12}H_{26}$ as fuel in order to prescribe the evaporation process. In fact, dodecane has a higher vapor pressure and a lower initial distillation temperature as compared with kerosene. Thus, it is relatively non-volatile and might reproduce the thermodynamical characteristics of kerosene [8].

Results

The numerical results concerning axial and turbulent kinetic energy using $k-\varepsilon$ and Reynolds Stress Model (Jones Musonge) are plotted in *Figure 2* and *Figure 3*. One observes a larger recirculation zone calculated with RSM turbulence model compared to $k-\varepsilon$. Differences are also observable on the axial velocity at the combustor exit. In these axial velocity plots, the air film coming from the z-rings, which are used to protect and cool the metallic shield in the primary and secondary zones, does not cover the entire outer part of the combustor. Note that all z-inlets represent multi-perforated wall. In order to accurately describe air injection through these cooling z-rings, it would be necessary to calculate each little air jet blowing from the drilled surface, but this method is obviously computationally too expensive. As an alternative solution one can apply a porous wall boundary condition, where the prescribed mass flux at the wall remains unchanged compared to a standard inlet condition. Unfortunately, the porous wall boundary condition is not available in the used code, i.e. the velocity components are adapted to satisfy the mass flux. The momentum flux is, therefore, not satisfied, due to the fact that the velocity entering the computational domain is much higher than the velocity based upon the surface averaged mass flow rate. This assumption could result in an overacted boundary condition since the total mass flux through all z-rings equals 35.19 %, which represent a considerable amount. Thereby it could exhibit an important influence on the flow field.

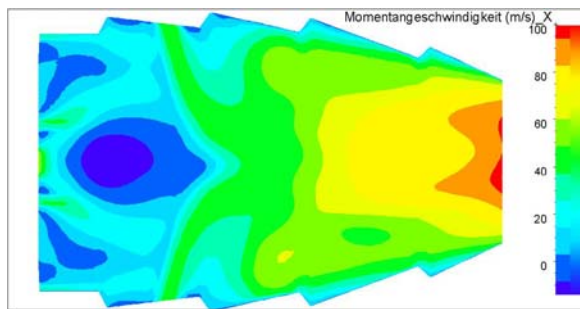


Figure 2: Axial velocity at the fuel injector plane (model)

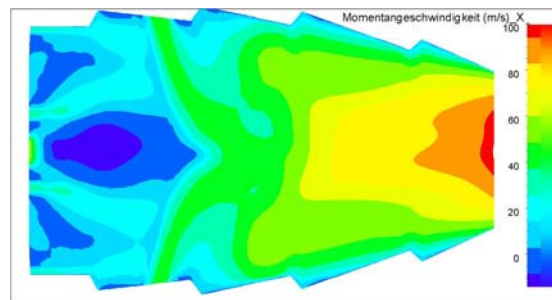


Figure 3: Axial velocity at the fuel injector plane (RSM(JM) model)

Figure 4 and *Figure 5* show plots of the turbulent kinetic energy (TKE). It can be seen that the maximum value of TKE is located in the centerline of the injector fuel plane where jets entering with 140 m/s through the mix-openings (see *Figure 1*) are going to meet. The predicted TKE by RSM model is higher than by $k-\varepsilon$ turbulence model, particularly in the secondary zone of the combustor where different jets are interacting. Contours of the turbulent kinetic energy suggest that small turbulent scales occur close to the combustor exit, whereas in the first zone of the flow field length scales are larger. Based on this observation, a parametric study on the influence of the swirl number at the inlet has been performed in order to enhance the turbulence intensity in the near fuel injector and thus seek optimum operating conditions.

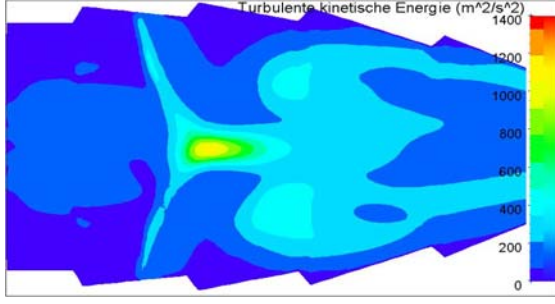


Figure 4: Turbulent kin. energy at the fuel injector plane ($k-\varepsilon$ model)

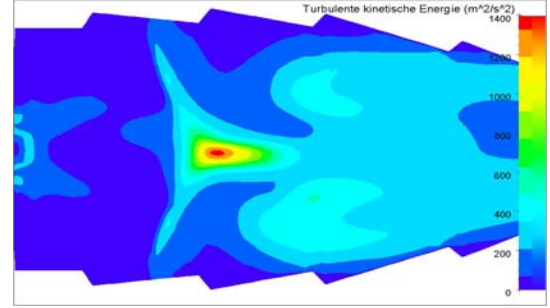


Figure 5: Turbulent kin. energy at the fuel injector plane (RSM(JM) model)

Concerning the spray behavior, one observes that droplets are nearly completely evaporated when they reach the first z-ring as shown in

Figure 6 and *Figure 7*. Results using RSM model show higher evaporation rate than $k-\varepsilon$ model. The spray seems to be deeply influenced by the carrier phase flow near the atomizer exit since its momentum is quite high in this region. In fact the big recirculation zone achieved by RSM model appears to be responsible for the differences of predicted evaporation rates. While using RSM model, droplets have to traverse a longer distance and thus recirculate for a longer period of time.

Another possible argumentation for different evaporation rates may be deduced from the turbulent kinetic energy (*Figure 4* and *Figure 5*). Having high values of TKE involve high fluid fluctuations at the droplet location, which in turn produce bigger relative velocity between droplets and carrier phase. The bigger the relative velocity the faster is the evaporation [8, 9].

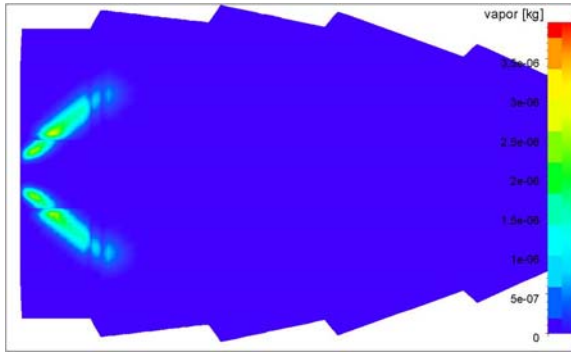


Figure 6: Vapor concentration at the fuel injector plane (model)

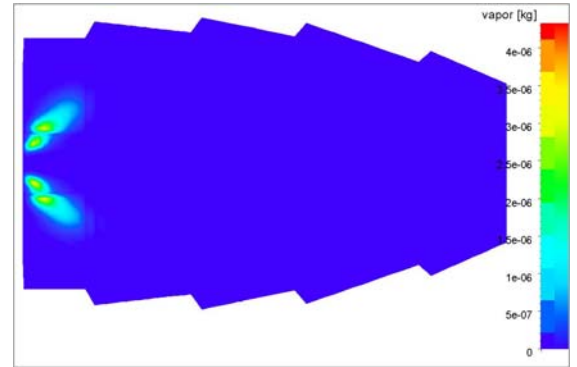


Figure 7: Vapor concentration at the fuel injector plane (RSM(JM) model)

Furthermore, one notices that the spray opening angle computed using $k-\varepsilon$ turbulence model is higher than that obtained with RSM. The radial velocity of the carrier phase computed by $k-\varepsilon$ turbulence model shows higher value than that achieved by RSM (see *Figure 8* and *Figure 9*). The droplets are dragged away by the gas flow towards the external wall.

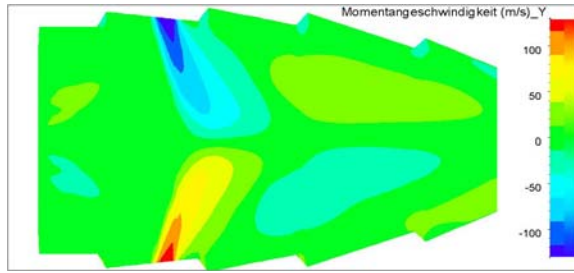


Figure 8: Radial velocity at the fuel injector plane ($k - \varepsilon$ model)

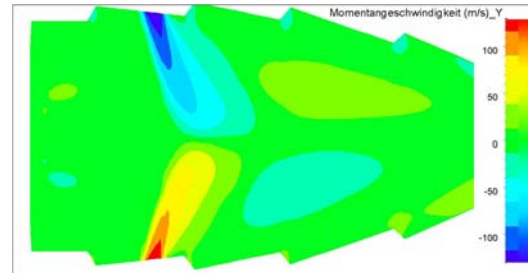


Figure 9: Radial velocity at the fuel injector plane (RSM(JM) model)

Conclusion

In this work, the effect of turbulence models on the prediction of spray evaporation at high pressure combustion chamber has been investigated. Within the spray module used, the uniform temperature model by Abramzon & Sirignano has been applied. Results show that the simulated evaporation rate using Reynolds Stress Model is higher than the one obtained by $k - \varepsilon$ turbulence model. This over-prediction of evaporation rate is due to a bigger recirculation zone achieved by RSM model as well as a higher value in turbulence intensity in the primary zone.

As future work, the evaporation model used in this paper is being extended to account for pressure that are close to critical value, e.g. for dodecane above 18 bars. Furthermore, suitable evaporation models for multi-component droplets have to be considered.

Acknowledgements

For financial support we gratefully acknowledge the Deutsche Forschungsgemeinschaft (DFG) through the Sonderforschungsbereich 568 (project A4)

References

- [1] Faeth G. M.: Evaporation and combustion of sprays: Progress in energy and combustion science, Pergamon Press, 9:1-76, 1983
- [2] Law C. K.: Unsteady droplet vaporization with droplet heating. Combustion and Flame, 26: 17-22, 1976
- [3] Oefelein J.C., Aggarwal S.K.: toward a unified high pressure drop model for spray simulation, center for turbulence research, Proceedings of summer program 2000, pp. 193-205
- [4] Prommersberger k, Stengele J, Dullenkopf K, Himmelsbach J and Wittig S "Investigations of droplet evaporation at elevated pressures" Collaborative Research Center 167, September 1998 Karlsruhe, Germany
- [5] Sirignano W. A.: "Fluid dynamics of sprays" 1992 Freeman Scholar Lecture J. Fluids Engng. Vol. 115, pp. 345-378. 1993
- [6] Crowe, C.T, Sommerfeld, M., Tsuji, Y., "Multiphase flow with droplets and particles", Boca Raton, Boston, New York, Washington, London. CRC Press LCC, 1998.
- [7] Smiljanovski V. and Brehm N. "CFD liquid spray combustion analysis of a single annular gas turbine combustor" ASME paper 99-GT-300 1999

- [8] Technical review aviation fuels. Chevron Business and Real Estate Services Creative Center, San Ramon, California. Aviation Fuels Technical Review (FTR-3) 2000 Chevron Products Company, A division of Chevron U.S.A. Inc.
- [9] Chrighui, M., Ahmadi, G., Sadiki, A., “Study on Interaction in Spray between Evaporating Droplets and Turbulence Using Second Order Turbulence RANS Models and a Lagrangian Approach”, Progress in Computational Fluid Dynamics, Special issue, 2004
- [10] Berlemont A., Grancher M.S. and Gouesbet G.: Heat and mass transfer coupling between vaporizing droplets and turbulence using a Lagrangian approach. J. of. Heat and Mass Transfer Vol.38 (1995) 3023-3034